Nature Geoscience manuscript NGS-2015-09-01665B

Riverine anaerobic ammonium oxidation across contrasting geologies

K. Lansdown,[1,2] B.A McKew,[3] C. Whitby,[3] C.M. Heppell[2], A.J. Dumbrell,[3] A. Binley,[4] L. Olde,[1] and M. Trimmer[1,*]

Affiliations:

1. School of Biological and Chemical Sciences, Queen Mary University of London, Mile End Road, London E1 4NS, United Kingdom.
2. School of Geography, Queen Mary University of London, Mile End Road, London E1 4NS, United Kingdom.
3. School of Biological Sciences, University of Essex, Wivenhoe Park, Colchester CO4 3SQ, United Kingdom.
4. Lancaster Environment Centre, Lancaster University, Lancaster, LA1 4YQ, United Kingdom

*Corresponding author: M. Trimmer, m.trimmer@qmul.ac.uk

Rivers are an important global sink for excess bioavailable nitrogen: they convert approximately 40% of terrestrial N-runoff per year (~47 Tg) to biologically unavailable N_2 gas and return it to the atmosphere.[1] Currently, riverine N_2 production is conceptualised and modelled as denitrification.[2-4] The contribution of anaerobic ammonium oxidation (or anammox), an alternate pathway of N_2 production important in marine environments, is not well understood.[5,6] Here we use *in situ* and laboratory measurements of anammox activity using ^{15}N tracers and molecular analyses of microbial communities to evaluate anammox in clay, sand, and chalk-dominated river beds in the Hampshire Avon catchment, UK during summer, 2013. Anammox *hzo* gene abundance varied across the contrasting geologies. Anammox rates were similar across geologies but contributed different proportions of N_2 production because of variation in denitrification rates. In spite of requiring anoxic conditions, anammox, most likely coupled to partial nitrification, contributed up to 58% of *in situ* N_2 production in oxic, permeable riverbeds. In contrast, denitrification dominated in low permeability clay-bed rivers, where anammox contributes roughly 7% to the production of N_2 gas. We conclude that anammox can represent an important nitrogen loss pathway in permeable river sediments.

Humans have greatly altered the global nitrogen cycle through industrial N_2 fixation and application of this fixed-N to the land, disturbing the balance between N_2 fixation and N_2 production.[1] Almost half of global terrestrial N_2 production occurs within freshwaters (rivers, lakes, groundwater)[2] which to date has been conceptualised as a simple function of labile organic matter availability, i.e. canonical denitrification.[4,7] Anammox alters the fundamental stoichiometry of the complete mineralisation of organic matter as, for every mole of organic-N converted to N_2, only half of the N-bearing compounds need partial oxidation to nitrite, and for each mole of nitrate/nitrite (NO_χ^-) reduced, one mole of more bioavailable

ammonium is also removed.[8] Rivers may not appear the most suitable environments for anammox – labile carbon,[9] supplied from the catchment, and variable redox environments[10] in the sediments, should, in theory, favour heterotrophic denitrification by facultative anaerobes.[11,12] If active however, anammox alters our perception of how riverbeds function and increases a river's capacity to attenuate nitrogen.

Much of what is known about anammox in the environment comes from estuaries and coastal seas where anammox varies in response to sediment reactivity. The relative contribution of anammox to marine N_2 production (*ra*) decreases with proximity to the shore as supply of carbon stimulates denitrification over anammox.[12,13] Extrapolating this trend further inshore suggested anammox activity would be insignificant in estuaries but anammox potential actually increased.[14,15] In both estuaries and coastal seas, however, anammox is important in low permeability sediments (*ra* <1 to 11 %)[9,16], where oxygen penetration is restricted[12,15] and it is these muddy sediments that the few studies of riverine anammox have occurred.[5,6] In addition, anammox is widespread in marine sediments but the affiliated bacteria are phylogenetically constrained. In contrast, freshwater environments have been shown to possess highest anammox diversity, purportedly containing many novel anammox bacteria.[17]

The geology of the Hampshire Avon catchment (United Kingdom) is dominated by permeable chalk from the Upper Chalk formation underlain by less permeable Upper Greensand and smaller outcrops of impermeable Gault clay (*see* Supplementary Information). Using a combination of *in situ* and laboratory-based ^{15}N tracer techniques[12,18] and molecular assays we characterised both the anammox community and its activity within rivers from clay, sand and chalk-dominated sub-catchments under summer, base flow conditions (Table S1). For rivers in which *in situ* measurements were performed we indexed catchment permeability by calculating the base-flow index (BFI, Table S2), the proportion of river flow

derived from deep groundwater sources. In clay catchments, low soil permeability leads to routing of rainfall overland or through shallow, more permeable soils into the river (low BFI). Whilst in chalk or sand catchments, the higher soil permeability allows infiltrated water to percolate deeper into the aquifer and follow much longer flow paths to towards the river (high BFI).

We began by characterising the anammox *hzo* functional gene that encodes hydrazine oxidoreductase which catalyses the oxidation of hydrazine to N_2. The *hzo* gene was detected in all sediments confirming that anammox bacteria were present (Table S3). Anammox activity was then confirmed by production of $^{29}N_2$ following addition of $^{15}NH_4^+$ and $^{14}NO_3^-$ to anoxic sediment slurries (Table S4). We can attribute this oxidation of ammonium to anammox rather than reduction of metal oxides,[19] for example, as no ^{15}N-N_2 was produced in $^{15}NH_4^+$ only controls (Table S4). Anammox potential varied across the riverine gradient with fastest rates and greatest anammox contribution to N_2 production observed in the permeable sands and chalk-gravels (Figure 1a, *see* Table S5). Anammox potential was also positively correlated with *hzo* gene abundance (r_s (7) = 0.867, p = 0.005). The absolute abundance of the *hzo* gene was significantly higher in chalk-gravels ($F_{(2,6)}$=8.64; p=0.017) and the proportion of *hzo* to 16S rRNA was even greater (Table S3), given that 16S rRNA copies were highest in the clays.

The anammox functional *hzo* gene was sequenced and phylogenetic analysis revealed four clades (Clade I-IV) that differed in their relative distributions between the three geologies. In general, there was a broad diversity of *hzo* sequences that were distinct from known *hzo* sequences (Figure S1a; Table S6; Supplementary discussion 1). In addition, we sequenced the 16S rRNA gene, and clustered 951,000 sequences into 28,000 OTUs. All Planctomycete sequences represented only 0.5-0.9% of the total 16S rRNA sequences, yet none were assigned to anammox genera (RDP classifier), or grouped phylogenetically with

any of the currently known anammox bacteria suggesting that anammox bacteria were not detected due to their low relative abundance in the bacterial communities (Table S3).

Somewhat surprisingly, ^{15}N-N_2 production was not limited to anoxic slurries as we also measured ^{15}N-N_2 production after addition of $^{15}NH_4^+$ to slurries with an air headspace (i.e. O_2 saturated; Figure 2, Figure S2). Sediments at the start of the incubation contained considerable $^{14}NH_4^+$ but little $^{14}NO_\chi^-$ (e.g. 350-960 μM and $\leq$3 μM, respectively; Table S7) which, in combination with $^{15}NH_4^+$, could result in $^{29}N_2$ and $^{30}N_2$ through either anammox or denitrification (or both) coupled to nitrification. As production of ^{15}N-N_2 happened immediately upon addition of $^{15}NH_4^+$ (Figure 2), nitrification must be rapid and the coupling to pathway(s) of N_2 production very tight. The potential for aerobic nitrification to fuel anammox has been demonstrated in oceanic waters with no measurable oxygen[20] and inferred in riparian soils.[21] Here we confirmed nitrifications' direct involvement in oxic N_2 production in sediments by addition of allylthiourea, an inhibitor of aerobic ammonium oxidation, which turned off N_2 production completely (Figure 2).

To apportion oxic N_2 production to coupled nitrification-anammox or nitrification-denitrification we modelled the distribution of isotopes within the N_2 produced via either pathway (*see* Methods). Despite clear evidence of nitrification within the slurries (*see* above), the majority of samples (31 of 45 incubations) did not have measurable $^{15}NO_\chi^-$ after the $^{15}NH_4^+$ addition (Table S7) and, therefore, coupling between nitrification and N_2 production was 100 % efficient. Without measurable NO_χ^- we can only assume that nitrification and N_2 production are so closely affiliated that the ^{15}N-content of the NO_χ^- and NH_4^+ pools are equal which, by definition, prevents separation of anammox from denitrification.[22] In the remaining incubations (n = 14; 5 and 9 for chalk-gravel and sand, respectively), $^{15}NO_\chi^-$ was detectable and the ^{15}N-labelling of the NO_χ^- and NH_4^+ pools was different. Production of ^{15}N-N_2 within the $^{15}NO_\chi^-$ -bearing subset of incubations was representative of the entire dataset (Figure S2);

120 although no $^{15}NO_\chi^-$ was detected within any clays (n = 15 time series, consisting of 75
121 discrete sediment samples).

122 We could apportion the production of N_2 gas to either anammox or denitrification in
123 some of the $^{15}NO_\chi^-$-containing experiments (n = 8 of 14), with 38±2 % and 65±15 % of
124 potential N_2 production occurring via anammox in the chalk-gravels and sands, respectively
125 (mean ± 1 s.e; Figure 2). Within the remaining $^{15}NO_\chi^-$-bearing experiments (n = 6 of 14), the
126 N_2 pool was more enriched in ^{15}N than could be explained by either denitrification or
127 anammox (deviation between measured and predicted ^{15}N-content of produced N_2 was 26±4
128 %, mean ± 1 s.e.; Table S8). This observation violates the assumption of a random
129 combination of isotopes which is fundamental to ^{15}N-assays and, for the N_2 to be more
130 enriched in ^{15}N than predicted, suggests heterogeneity in the ^{15}N labelling of substrate
131 pool(s).[23] Here, the heterogeneity probably exists because the NO_2^- pool actually being
132 reduced is partially physically isolated from the bulk NO_χ^- pool, further supporting a tight
133 coupling of nitrification to N_2 production. Heterogeneity in the NH_4^+ pool is less likely as
134 ammonium was plentiful – both as ambient $^{14}NH_4^+$ (Table S7) and added $^{15}NH_4^+$ (500 μM 98
135 % ^{15}N).

136 Supply of nitrite rather than ammonium has been suggested as the limiting factor for
137 anammox in aquatic sediments – potentially coupling anammox to either nitrification and/or
138 denitrification.[15] In anoxic marine and estuarine sediments, anammox can be fuelled by
139 denitrification-derived nitrite[15], even forming a symbiotic relationship with some nitrate
140 reducing / sulphur oxidising bacteria.[24] Association between nitrifiers and anammox bacteria
141 may be weak in low permeability sediments (clays, estuarine mud) because much of the
142 nitrite produced in the upper few millimetres of the bed can diffuse into the overlying water
143 or be fully oxidised to nitrate before reaching the sub-oxic layer.[15] In the presence of oxygen
144 however, affinity between nitrifiers and anammox bacteria can exist in aggregates and is

indeed the fundamental principle of CANON waste-water treatment reactors operating at reduced oxygen.[25] The ability for anammox bacteria to couple to both aerobic and anaerobic pathways of nitrite production could be very advantageous in permeable riverbeds, where groundwater-surface exchange facilitates advective transport of solutes,[26] creating a mosaic of redox micro-environments[27] within which both nitrification and denitrification can occur.[18]

Rates of *in situ* anammox activity were similar across riverbeds of differing geology (Figure 1b), despite large differences in porewater oxygen – clays were essentially anoxic whilst oxygen was present in both the sand and chalk-gravels (8 to 110 % of air-equilibration; mean ± 1 s.e. = 134±14 μM; Figure S3). In contrast, anammox did make a markedly higher contribution to N_2 production in the permeable sediments compared to the clays (Figure 1b, Table S5); not because anammox activity increased, rather that denitrification activity declined (Table S9). Similar increases in the significance of anammox at the expense of denitrification are well documented in marine sediments.[12] Differences in *ra* between clays, sands and chalk-gravels were consistent across seasons (Figure S5) and are related to the chemical gradient inherent to porewaters of these different riverbed types. Within clays, porewaters were typically reduced (high in ammonium, iron (II) and phosphate) whereas chalk-gravel porewaters were more oxidised (high in nitrate, intermediate in O_2; Figure S4) with *ra* increasing as porewaters become more oxidised (Figure 3a; r_s (38) = -0.73, p<0.001); hinting at a potential coupling between anammox and nitrification. Anammox activity was strongly associated with nitrite and O_2, increasing as nitrite accumulates in partially oxygenated sediments (Figure 3b) – again mirroring the coupling between partial nitrification and anammox in aggregates as exploited in CANON reactors.[25] In contrast, anammox activity had essentially no association with ammonium, as where ammonium accumulates in these riverine sediments, labile organic carbon (the source of the ammonium) must also be plentiful (Figure 3b), fuelling denitrification at the expense of anammox.[12,13] Overall we found a very

strong increase in the contribution of anammox to N_2 production and *hzo* abundance (as a fraction of total bacteria, *hzo*:16S rRNA sequences) with increasing BFI (r_s (6) = 1.0, p = 0.003 and r_s (6) = 1.0, $p < 0.001$ for anammox contribution and *hzo* abundance, respectively; Figure 3c), suggesting, in the long-term, that anammox is favoured with stable conditions (nutrients, temperature, pH).[11]

Here, we have shown how anammox is making a significant contribution to the removal of fixed-N in oxic, permeable riverbeds; a pattern completely at odds with current knowledge. Supply of nitrite to anammox from partial nitrification removes the stoichiometric constraint of denitrification-anammox coupling (*ra* ≤29 %),[28] allowing anammox to potentially be as important an N-sink as denitrification in permeable riverbeds (maximum *in situ ra* = 58 %, median = 37 % for chalk-gravels; Figure 3a). In the clays, anammox proceeds as per muddy estuarine sediments, making only a minor contribution to N_2 production (*ra* ≤7 %) and being fuelled by canonical denitrification.[15] It is important to appreciate that the stoichiometry of anammox, requiring only partial oxidation of some N-substrates, increases the efficiency of rivers to remove fixed N as both NO_χ^- and ammonium, changing our understanding of the ecosystem services they provide.

Data sources

URL and DOI for activity data to be provided once deposition into the Environmental Information Data Centre is complete. *hzo* gene sequences from this study are deposited in GenBank (NCBI) under the accession numbers ---

References

1 Galloway, J. N. *et al.* Nitrogen cycles: past, present, and future. *Biogeochemistry* **70**, 153 - 226 (2004).

195 2 Seitzinger, S. *et al.* Denitrification across landscapes and waterscapes: a synthesis.
196 *Ecol. Appl.* **16**, 2064-2090 (2006).
197 3 Burgin, A. J. & Hamilton, S. K. Have we overemphasized the role of denitrification in
198 aquatic ecosystems? A review of nitrate removal pathways. *Front. Ecol. Environ.* **5**,
199 89 - 96 (2007).
200 4 Piña-Ochoa, E. & Álvarez-Cobelas, M. Denitrification in Aquatic Environments: A
201 Cross-system Analysis. *Biogeochemistry* **81**, 111-130 (2006).
202 5 Zhou, S., Borjigin, S., Riya, S., Terada, A. & Hosomi, M. The relationship between
203 anammox and denitrification in the sediment of an inland river. *Sci. Total Environ.*
204 **490**, 1029-1036 (2014).
205 6 Zhao, Y. *et al.* Seasonal variation and controlling factors of anaerobic ammonium
206 oxidation in freshwater river sediments in the Taihu Lake region of China.
207 *Chemosphere* **93**, 2124-2131 (2013).
208 7 Taylor, P. G. & Townsend, A. R. Stoichiometric control of organic carbon-nitrate
209 relationships from soils to the sea. *Nature* **464**, 1178-1181 (2010).
210 8 van de Graaf, A. A. *et al.* Anaerobic oxidation of ammonium is a biologically
211 mediated process. *Appl. Environ. Microb.* **61**, 1246-1251 (1995).
212 9 Gihring, T. M., Canion, A., Riggs, A., Huettel, M. & Kostka, J. E. Denitrification in
213 shallow, sublittoral Gulf of Mexico permeable sediments. *Limnol. Oceanogr.* **55**, 43-
214 54 (2010).
215 10 Trimmer, M., Engström, P. & Thamdrup, B. Stark Contrast in Denitrification and
216 Anammox across the Deep Norwegian Trench in the Skagerrak. *Appl. Environ.*
217 *Microb.* **79**, 7381-7389 (2013).

11 Rysgaard, S., Glud, R. N., Risgaard-Petersen, N. & Dalsgaard, T. Denitrification and anammox activity in Arctic marine sediments. *Limnol. Oceanogr.* **49**, 1493-1502 (2004).

12 Thamdrup, B. & Dalsgaard, T. Production of N_2 through anaerobic ammonium oxidation coupled to nitrate reduction in marine sediments. *Appl. Environ. Microb.* **68**, 1312 - 1318 (2002).

13 Engström, P., Dalsgaard, T., Hulth, S. & Aller, R. C. Anaerobic ammonium oxidation by nitrite (anammox): implications for N_2 production in coastal marine sediments. *Geochim. Cosmochim. Acta.* **69**, 2057 - 2065 (2005).

14 Nicholls, J. C. & Trimmer, M. Widespread occurrence of the anammox reaction in estuarine sediments. *Aquat. Mircob. Ecol.* **55**, 105 - 113 (2009).

15 Meyer, R. L., Risgaard-Petersen, N. & Allen, D. E. Correlation between anammox activity and microscale distribution of nitrite in a subtropical mangrove sediment. *Appl. Environ. Microb.* **71**, 6142 - 6149 (2005).

16 Trimmer, M., Nicholls, J. C. & Deflandre, R. Anaerobic ammonium oxidation measured in sediments along the Thames Estuary, United Kingdom. *Appl. Environ. Microb.* **69**, 6447 - 6454 (2003).

17 Sonthiphand, P., Hall, M. W. & Neufeld, J. D. Biogeography of anaerobic ammonia-oxidizing (anammox) bacteria. *Front. Microbiol.* **5** (2014).

18 Lansdown, K. *et al.* Fine-Scale in Situ Measurement of Riverbed Nitrate Production and Consumption in an Armored Permeable Riverbed. *Environ. Sci. Technol.* **48**, 4425-4434 (2014).

19 Luther III, G. W., Sundby, B., Lewis, B. L., Brendel, P. J. & Silverberg, N. Interactions of manganese with the nitrogen cycle: Alternative pathways to dinitrogen. *Geochim. Cosmochim. Acta.* **61**, 4043-4052 (1997).

20 Lam, P. *et al.* Linking crenarchaeal and bacterial nitrification to anammox in the Black Sea. *Proceedings of the National Academy of Sciences* **104**, 7104-7109 (2007).

21 Zhu, G. *et al.* Hotspots of anaerobic ammonium oxidation at land-freshwater interfaces. *Nature Geosci.* **6**, 103-107 (2013).

22 Spott, O. & Stange, C. F. A new mathematical approach for calculating the contribution of anammox, denitrification and atmosphere to an N_2 mixture based on a ^{15}N tracer technique. *Rapid Commun. Mass Sp.* **21**, 2398-2406 (2007).

23 de Brabandere, L. *et al.* Vertical partitioning of nitrogen-loss processes across the oxic-anoxic interface of an oceanic oxygen minimum zone. *Environ. Microbiol.* **16**, 3041-3054 (2014).

24 Prokopenko, M. G. *et al.* Nitrogen losses in anoxic marine sediments driven by *Thioploca*-anammox bacterial consortia. *Nature* **500**, 194-198 (2013).

25 Sliekers, A. O. *et al.* Completely autotrophic nitrogen removal over nitrite in one single reactor. *Water Res.* **36**, 2475 - 2482 (2002).

26 Brunke, M. & Gonser, T. The ecological significance of exchange processes between rivers and groundwater. *Freshwater Biol.* **37**, 1 - 33 (1997).

27 Baker, M. A., Dahm, C. N. & Valett, H. M. Acetate retention and metabolism in the hyporheic zone of a mountain stream. *Limnol. Oceanogr.* **44**, 1530 - 1539 (1999).

28 Dalsgaard, T., Canfield, D. E., Petersen, J., Thamdrup, B. & Acuna-Gonzalez, J. N_2 production by the anammox reaction in the anoxic water column of Golfo Dulce, Costa Rica. *Nature* **422**, 606-608 (2003).

Correspondence and requests for materials should be addressed to M.T.

Acknowledgements

This study was funded through the Natural Environment Research Council (NERC) Macronutrient cycles program. B. McKew's contribution was also part-funded by the Eastern Academic Research Consortium (Eastern ARC). We acknowledge the land owners for allowing us access to the rivers studied. Collection and preparation of sediment was assisted by S.Warren, I. Sanders, F. Shelley and V. Warren. The comments from R. Glud, three anonymous reviewers and the associate editor have helped strengthen this manuscript.

Author contributions

MT with CMH, AB and KL conceived the original project. KL performed ^{15}N-related work and with MT interpreted the process data and drafted the original manuscript. BAM designed and performed all the molecular work and phylogenetic analysis. AJD constructed the bioinformatic pipeline and performed the NGS analysis. CW directed the molecular component of project. LO assisted with fieldwork and performed sediment characterisation. AB and CMH performed hydrologic measurements and calculated base-flow indices. All authors contributed to writing the paper and approved the final manuscript.

Competing financial interests

The authors declare no competing financial interests.

287 **Figure Captions**

288 **Figure 1: Anammox activity, both rate and contribution to N_2 production (*ra*), differs**
289 **across a riverine gradient.** Activity was measured as total potential in anoxic slurries **(a)**
290 and ambient rates by direct, *in situ* measurements (*see* Supplementary Methods) **(b)**. Grey
291 bars indicate significant differences between groups. Data are mean values ±1 standard error
292 (n = 5 and 10 for **a** and **b**, respectively).

293

294 **Figure 2: Production of ^{15}N-labelled N_2 following addition of $^{15}NH_4^+$ to chalk-gravels (a)**
295 **and sand (b) incubated under air-saturated conditions.** Notice that in the presence of
296 allylthiourea (white circles), an inhibitor of nitrification, there was no production of ^{15}N-N_2
297 but without the inhibitor (black circles) there was immediate conversion of $^{15}NH_4^+$ to ^{15}N-N_2
298 confirming the tight coupling between nitrification and N_2 production. Grey boxes are
299 dissolved O_2. The pathways of N_2 production (anammox or denitrification, red versus white
300 column sections, respectively) were determined via modelling (*see* Supplementary Methods).
301 Data are mean values ±1 standard error (n = 5).

302

303 **Figure 3: Anammox varies with both patch scale and sub-catchment river**
304 **characteristics.** Differences in anammox contribution to *in situ* N_2 production within clays
305 (red, n=10), sands (blue, n=20) and chalk-gravels (yellow, n=20) result from fine-scale
306 chemical variation **(a)** (lower scores are more oxidised porewaters, *see* Figure S4). Anammox
307 activity is most strongly associated with nitrite and O_2 **(b)**. Squares represent geology
308 averages in the redundancy-analysis triplot. At the sub-catchment scale, both anammox
309 contribution and bacterial abundance (*hzo* copy number: total bacteria) increase markedly
310 with increasing base-flow index **(c)**. Data are means ±1 standard error (n = 3 for *hzo*
311 fractions).

312

Methods

Measurement of potential anammox activity

Collection of sediment. Sediment was collected from nine rivers in the Hampshire Avon catchment in summer 2013 (19-20 August) under base flow conditions. Rivers were in sub-catchments of predominantly clay, sand or chalk (n = 3 per geology). Full site descriptions are provided as supplementary information. At each river, surficial sediments (<5 cm) were removed from five un-vegetated patches of the main channel by hand with Perspex cores (internal diameter = 9 cm). After sediment disturbed within the core settled, the overlying water was gently decanted and sediment for activity measurements was placed in ziplock bags and stored at ~4 °C.

Preparation of slurries. In the laboratory, each bag of sediment was homogenised by gentle stirring and particles > 9 mm (the internal diameter of the vials) were removed. Sediments were then placed in pre-weighed gas-tight vials (Exetainer, Labco) with replicates from the rivers treated as discrete samples. Slurries were prepared with synthetic river water (*see* supplementary information) in a 1:1 sediment-to-water ratio.

The potential for anammox and denitrification was measured in anoxic slurries[29-31] (oxygen-free N_2 headspace, British Oxygen Company) prepared with de-oxygenated synthetic river water in an anoxic hood (CV24, Belle Technologies). Anoxic slurries were pre-incubated in the dark on an orbital shaker (80 r.p.m., Stuart SSL1) for at least 18 hours to remove any ambient $^{14}NO_{\chi}^{-}$. ^{15}N tracers (100 µL, de-oxygenated) were injected through the septa of the vials in the following combinations: $^{15}NH_4^+$ only, $^{15}NH_4^+$ and $^{14}NO_3^-$ and $^{15}NO_3^-$ only. All ^{15}N-salts were 98 atom % ^{15}N (Sigma-Aldrich). Tracers increased ammonium concentrations by 500 µM and nitrate concentrations to 100 or 300 µM in the clay and permeable sediments, respectively. Each sediment and treatment combination consisted of a reference (no tracer added) and a killed control (100 µL 7M $ZnCl_2$ injected prior to the

338 tracer). The $^{15}NO_3^-$ treatment consisted of 5 additional slurries per sample which were
339 incubated for 0.5, 1, 2, 3 and 6 h on an orbital shaker (as above). The $^{15}NH_4^+$ and $^{15}NH_4^+$ and
340 $^{14}NO_3^-$ treatments were end point only experiments with 1 additional slurry per sample (i.e.
341 T_{final}) incubated for 6 h. At the end of the incubation period, biological activity was stopped
342 by injection of $ZnCl_2$ (as above) and gas-tight vials were stored upside down until analysis.
343 Once headspace analysis was complete (*see* below) vials were opened and water extracted
344 after centrifugation. Sediment was re-suspended twice with ultrapure water (same volume as
345 aqueous phase of slurry) and the supernatant reserved. Water samples were filtered (0.45 µm
346 polypropylene, Gilson Scientific) into plastic tubes (polypropylene, VWR International) and
347 frozen until analysis (*see* below). The mass of sediment within each vial was then determined
348 after sediments had been dried.

349 A parallel set of oxic slurries (air headspace) were prepared to investigate nitrification
350 potential by addition of air-equilibrated synthetic river water to sediments on the lab bench
351 with no pre-incubation. Air-equilibrated $^{15}NH_4^+$ tracer was injected through the septa of the
352 vials (as above) and slurries were treated as per the anoxic $^{15}NO_3^-$ treatment. A second
353 experiment was devised to examine if N_2 production observed in the oxic slurries was linked
354 to nitrification (Rivers Ebble and Nadder only, 8/11/2013, sampling procedures as above). In
355 addition to the $^{15}NH_4^+$ treatment, a second treatment containing both $^{15}NH_4^+$ and allylthiourea
356 (concentration in slurry = 100 µM), a nitrification inhibitor, was also included. To determine
357 if oxygen depletion occurred within the oxic slurries a set of scaled-up slurries were prepared
358 in 20 mL gas-tight vials (Chromacol). At each time point the vial was opened and the
359 dissolved O_2 concentration of the slurry was measured by inserting a calibrated, fast response
360 micro-electrode (50 µm, Unisense).
361

362 **Measurement of in situ anammox activity**

363 Impermeable sediments. Ambient rates of anammox and denitrification were estimated in un-
364 vegetated clays by incubation of $^{15}NO_3^-$ in intact sediment cores[32] (Perspex cores with rubber
365 bungs, internal diameter = 3.4 cm, experiments performed between 03/08 and 10/08/2013).
366 Cores were collected by hand from the River Sem (*n*= 34) and a tributary of the River Sem
367 (Clay 2 in Table S1, *n*= 29) and incubated on site in a tank full of river water. The amount of
368 $^{15}NO_3^-$ added and the duration of the incubation varied between cores, ranging from 0.05 to
369 2.5 mL of 78 mM $^{15}NO_3^-$ (98 atom % ^{15}N) and 31 to 252 minutes respectively. The range in
370 $^{15}NO_3^-$ amendments aided separation of anammox from denitrification[32] and different
371 incubation times were used to verify ^{15}N-N_2 production was linear. Following $^{15}NO_3^-$
372 injection into the overlying water column, cores were immediately capped with a bung fitted
373 with a magnetic stirrer and placed in the incubation tank. The overlying water column was
374 gently stirred to prevent stratification and light was excluded from the incubation tank. At the
375 end of the incubation the bung was removed from the core and a water sample was quickly
376 withdrawn with a syringe (polypropylene, BD Plastipak). The core was then homogenised by
377 gentle stirring and decanted into a gas-tight vial (12 mL Exetainer, Labco) which was
378 allowed to overflow before being capped. Biological activity was stopped by injection of
379 100 µL of formaldehyde through the septum. The water sample was then filtered and frozen
380 (as above) until later analysis. Four additional sediment cores were retrieved on each day of
381 fieldwork and a water sample and slurrified sample collected (as above) to determine ambient
382 ^{15}N-N_2 concentrations.

383 Ambient chemistry within the clays was determined on porewaters recovered using
384 rhizon samplers[33] (0.2 µm mesh, 10 cm screen, Rhizosphere) inserted into the riverbed.
385 Rhizon samplers were allowed 24 h to pre-equilibrate[34] before porewater was extracted by
386 applying a vacuum to the rhizon sampler via a syringe held open with a spacer bar. Water

samples for nutrient analysis were processed as described above. Water samples for iron (II) determination were preserved by dispensing porewater directly into a solution of buffered phenanthroline[35] (3.5:1 1M pH 4.5 Acetate buffer: 0.2 % (w/v) 1-10-phenanthroline monohydrate). The dissolved O_2 concentration of the recovered porewater was measured by placing the O_2 microelectrode (as above) into an empty syringe barrel and gently transferring porewater into the vessel with a 2-way valve.[36] We estimate that sample collection and transfer adds approximately 10 μM O_2 to the actual dissolved O_2 concentration and corrected all values accordingly. Following measurement of dissolved O_2 the pH was determined (pH100, VWR International). Additional sediment cores (Perspex, 9 cm diameter) were collected and transported back to the laboratory for fine scale oxygen profiling using a Clark-type oxygen microsensor (OX50, Unisense) within an automated micromanipulator controlled by microprofiling software (SensorTracer PRO, Unisense). Readings from the microelectrode were displayed on a picoammeter (PA 2000; Unisense) and logged after 4 s when the signal had stabilized.

Permeable sediments. Ambient rates of anammox and denitrification were estimated in un-vegetated sediments of the Rivers Ebble, Wylye, Nadder and Avon ("Sand 2" in Table S1) by injection of $^{15}NO_3^-$ into the riverbed and collection of samples over time (i.e. "push-pull" sampling; sampling occurred between 31/07 and 15/08/2013). Ten bespoke stainless steel mini-probes were installed between 4 and 20 cm depth in the bed of the main channel on the day prior to the injection. We modified the system from previous work [36] by attaching an extension (1 m length of 0.75 mm internal diameter Polyetheretherkeytone (PEEK) tubing, Polyflon Technology Ltd.) to the luer connector of the mini-probe to improve speed of sampling. Prior to the injection of $^{15}NO_3^-$, porewater (15 mL total) was withdrawn from each mini-probe for dissolved O_2 and pH measurement, nutrient and iron (II) analysis and natural

411 abundance ^{15}N-N_2 (as above). Gas samples were collected in 3 mL gas-tight vials and
412 poisoned with $ZnCl_2$ (25 µL, as above).

413 A tracer solution consisting of 300 µM $^{15}NO_3^-$ (98 atom % ^{15}N) in a synthetic river
414 water/ KCl (4 mM) matrix, was de-oxygenated (as above) and 25 mL aliquots were drawn
415 into luer-lock syringes. Tracer was injected into the riverbed via the mini-probes, with each
416 injection lasting ~20 seconds. Porewater was recovered from each mini-probe immediately
417 post injection and a dissolved gas and water sample was collected (as above). Porewater was
418 then recovered at ~5, 10 and 30 minutes post injection and sampled as above.
419

420 **Analytical methods for activity measurements**

421 Nitrate (Limit of detection (LOD) 0.4 µM, precision 1 %), nitrite (LOD 0.1 µM, precision
422 1 %), ammonium (LOD 0.8 µM, precision 3 %) and soluble reactive phosphate (SRP, LOD
423 0.1 µM, precision 1 %) were quantified by automated colorimetric analysis using standard
424 methods (San++, Skalar). Iron(II) concentrations were quantified on samples preserved with
425 buffered phenanthroline[35] by absorbance measurement at 520 nm on a UV/Visible
426 spectrophotometer (LOD 1 µM, precision 1 %; Evolution 100, Thermo Fisher). The dissolved
427 oxygen electrode was calibrated with a zero solution (0.1 M sodium ascorbate in 0.1 M
428 sodium hydroxide) and 100% air-equilibrated water (laboratory measurements) or river water
429 (field-based measurements), the dissolved O_2 concentration of which was later determined by
430 Winkler titration. Samples for ^{15}N-N_2 quantification that did not contain a headspace were
431 prepared for analysis by addition of helium (commercially pure grade, British Oxygen
432 Company) with a syringe and a two-way valve (0.5 or 2 mL headspaces were added to
433 porewater and slurrified core samples, respectively) and were equilibrated at 22 °C overnight
434 on an orbital shaker (as above). The isotopic composition of N_2 was determined by injection
435 of 50 or 100 µL of headspace (porewater and core/slurry samples, respectively; CombiPAL,

436 CTC Analytics) into a continuous flow isotope-ratio mass spectrometer (Delta Plus,
437 ThermoFinnigan) and measurement of mass-to-charge ratios 28, 29 and 30. Further details of
438 calibration are provided as supplementary information. Samples for N_2O determination were
439 prepared by withdrawing a sub-sample of the headspace described above (100 μL for
440 porewater samples and 1-10 μL for slurrified core samples) and injecting it into a gas-tight
441 vial containing 2 nmoles of N_2O (prepared by dilution of 100 % N_2O in a N_2 matrix, British
442 Oxygen Company). The entire contents of these vials was swept into a trace-gas pre-
443 concentrator module (Cryo-Focusing, Precon, ThermoFinnigan) and mass-to-charge ratios
444 44, 45 and 46 were measured on the mass spectrometer described above. Samples for $^{15}NO_\chi^-$
445 determination were prepared by reduction of nitrate to nitrite with spongy cadmium
446 (modified from ref. 37 - 5 mL of sample and 0.2 mL of 1 M Imidazole were used and
447 samples were incubated for 2 h on an orbital shaker, as above). Samples were then transferred
448 to gas-tight vials (3 mL Exetainer, Labco) and a 0.5 mL helium headspace was added (as
449 above). Nitrite was reduced to N_2 by injection of sulphamic acid through the septa (100 μL 4
450 mM sulphamic acid in 4 M HCl; B. Thamdrup, personal communication) and, after overnight
451 equilibration, the headspace was analysed for ^{15}N-N_2 as above. The amount of $^{15}NO_\chi^-$ within
452 each vial was determined by preparation of a calibration curve of differing amounts of $^{15}NO_3^-$
453 (treated as above) versus the mass-to-charge ratio 29: sum of all areas.
454
455 **Calculations for activity measurements**
456 Production of ^{15}N-N_2, anammox and denitrification potential in anoxic slurries were
457 calculated using standard procedures.[30] Rates of ambient anammox and denitrification were
458 calculated using methods previously applied to intact sediment cores with differences in the
459 ^{15}N-labelling of the N_2 and N_2O pools used to determine the contribution of anammox.[32] In
460 oxic slurries, anammox and denitrification were apportioned by comparing the proportion of

461 ^{15}N in the produced N_2 to anammox and denitrification endmembers in a mixing model. All
462 calculations used to derive rates, contribution of anammox to N_2 production and other
463 parameters (e.g. base flow index) are provided as supplementary information.
464
465 **Statistical methods for activity measurements**
466 All statistics were performed in R[38] (version 3.1.1) using RStudio[39] (version 0.98.1091).
467 Differences in anammox activity between groups was tested with linear mixed effects models
468 using the nlme package[40] where geology or permeability were fitted as fixed effects and site
469 was a random effect.[41] Model fit was improved by adding variance structure to the model
470 allowing variance to differ between groups. Significance of fixed effects ($p < 0.05$) were
471 determined by log likelihood ratio tests between the model of interest and a reduced model,[41]
472 i.e. with no fixed effect but just a random intercept (*see* Table S5).
473 The effect of porewater chemistry on anammox and denitrification was examined
474 using multivariate techniques. First we used principal component analysis (PCA) to
475 investigate correlations between chemical variables and differences in porewater chemistry
476 between rivers. The PCA reduced 7 chemical variables (nitrate, nitrite, ammonium, dissolved
477 O_2, SRP, iron (II) and pH) to two principal components (total variance explained = 74%).
478 Principal component 1 accounted for 56 % of the variance and comprised strong positive
479 loadings for ammonium, Iron (II) and SRP, strong negative loadings for nitrate and pH and
480 an intermediate negative loading for O_2 (Figure S4). We have interpreted this axis as a
481 chemical gradient moving from reduced porewaters, where mineralisation products such as
482 ammonium and SRP accumulate (high scores), to oxidised porewaters (low scores) high in
483 nitrate and intermediate in O_2. The chemistries captured within PC1 separate data into their
484 respective geologies (Figure S4), essentially converting our categorical "gradient" of
485 permeability (i.e. clay, sand or chalk) into a true riverine gradient. PC2 was most strongly

associated with oxygen (positive) and nitrite (negative, Figure S4), however, this axis only explained 19 % of the variance.

We then performed a redundancy analysis using the vegan package[42] with the same chemical dataset, geology as a grouping factor and response variables ambient anammox and denitrification rates and the contribution of anammox to N_2 production (*ra*). We attempted to determine the most parsimonious model by performing stepwise addition of the variables, however, after inclusion of the factor "geology" there were no significant improvements to the model Akaike Information Criterion. Geology alone, i.e. sand or clay, is not very useful for determining chemical controls on riverine anammox but when removed from the model the goodness of fit was considerably reduced (>11% reduction observed). We therefore determined the most parsimonious model by manually comparing adjusted R^2 values following the addition of chemical variables.[43] The explanatory variables of the simplest model were found to be geology, ammonium, nitrate, nitrite and O_2 (Figure 3b, Adjusted R^2 = 0.40). In this simplest model 78 % of the variance was explained by the 1st canonical axis which had similar chemical loadings as PC1 in the original PCA.

Relationships between anammox and other variables (e.g. *hzo* gene copy number) were quantified using Spearman's rank correlation on untransformed data with $p<0.05$ used as the criteria for significance.

Molecular analyses

Collection of sediment. Sediment collected for potential anammox activity (see above) was sub-sampled for molecular analysis (n=3 for the 9 rivers sampled). Sediment was placed in sterile tubes and preserved cryogenically at -150°C.

qPCR gene abundance. DNA was extracted from 0.25 g wet weight sediment using PowerSoil® DNA Isolation Kit (MO BIO Laboratories, Inc). Gene abundance was

quantified by qPCR with SensiFAST SYBR No-ROX Kit (Bioline) on a CFX96 Real-Time PCR Detection System (BioRad) using the 16S rRNA primer pair Bakt_341F (CCTACGGGNGGCWGCAG) and Bakt_805R (GACTACHVGGGTATCTAATCC)[44] and the *hzo* primer pair HZO-1F (AAGACNTGYCAYTGGGGWAAA) and HZO-1R (GACATACCCATACTKGTRTANACNGT).[45] Gene abundances were quantified by absolute quantification method against an internal standard calibration curve of DNA standards of the target gene from 10^2 to 10^6 copies in 20 µl reactions containing 400 nM of primers and 1 µl of DNA template. Cycle conditions were 95 °C for 2 min followed by 40 cycles at 95 °C for 10s then 60 °C for 30 seconds. Amplification of a single product was confirmed by melting curve analysis.

Amplicon sequencing. Amplicon libraries were prepared by a 28-cycle PCR using primers containing the same target region as the qPCR primers but flanked with Illumina Nextera overhang sequences. Amplicons were purified using AMPure XP (Agencourt) SPRI bead protocols, before adding Illumina flowcell adapter sequences, and one of 96 unique combinations of Nextera paired-end Indexes via a 8-cycle PCR. Amplicons were again purified using AMPure XP beads, quantified using a Quant-iT Picogreen dsDNA assay kit (Life Technologies) on a Nanodrop 3300 fluorospectrometer (Thermo Scientific) and then pooled in equimolar concentrations. The amplicon libraries were quality checked using a DNA 1000 kit on at 2100 Bioanalyzer (Agilent) before sequencing was performed on the Illumina Miseq platform using a MiSeq reagent kit V3 (2 × 300 bp) at TGAC (The Genome Analysis Centre, Norwich). The sequencing reads were analysed using the QIIME pipeline and associated modules.[46] Sequences were de-multiplexed using the Nextera Indexes and quality filtered to remove sequences below Q20 or that contained, any errors in the primer region, above 6 ambiguous bases, and chimeras. The quality filtered reads were clustered into operational taxonomic units (OTUs) using the USEARCH algorithm[47] at the 0.95 level (*hzo*)

or 0.97 level (16S rRNA). 16S rRNA representative sequences from each OTU were assigned taxonomic identities with the RDP classifier.[48] Statistical analysis was performed in the R statistical language version 3.1.3 using the R base libraries[38] and the community ecology analysis- specific package 'vegan'.[42] *hzo* gene multiple sequence alignment was performed on the 100 most abundant OTUs (representing 92-93 % of all sequences in each geology) and codon aligned deduced amino acid seqeunces using MUSCLE (**MU**ltiple **S**equence **C**omparison by **L**og- **E**xpectation)[47] and phylogenies were constructed in MEGA6[49] The nucleotide sequence evolutionary history was inferred by using the Maximum Likelihood method based on the General Time Reversible model.[50] Initial trees for the heuristic search were obtained by applying the Neighbor-Joining method to a matrix of pairwise distances estimated using the Maximum Composite Likelihood (MCL) approach. A discrete Gamma distribution was used to model evolutionary rate differences among sites. The amino acid evolutionary history was inferred by using the Maximum Likelihood method based on the Le and Gascuel 2008 model.[51] Initial tree(s) for the heuristic search were obtained automatically by applying Neighbor-Join and BioNJ algorithms to a matrix of pairwise distances estimated using a JTT model, and then selecting the topology with superior log likelihood value. A discrete Gamma distribution was used to model evolutionary rate differences among sites. Significance of branching order was determined by bootstrap analysis (1000 replicates).[52]

References for methods

29 Trimmer, M., Nicholls, J. C. & Deflandre, R. Anaerobic ammonium oxidation measured in sediments along the Thames Estuary, United Kingdom. *Appl. Environ. Microbiol.* **69**, 6447 - 6454 (2003).

30 Thamdrup, B. & Dalsgaard, T. Production of N_2 through anaerobic ammonium oxidation coupled to nitrate reduction in marine sediments. *Appl. Environ. Microbiol.* **68**, 1312 - 1318 (2002).

31 Engström, P., Dalsgaard, T., Hulth, S. & Aller, R. C. Anaerobic ammonium oxidation by nitrite (anammox): implications for N_2 production in coastal marine sediments. *Geochim. Cosmochim. Acta.* **69**, 2057 - 2065 (2005).

32 Trimmer, M., Risgaard-Petersen, N., Nicholls, J. C. & Engström, P. Direct measurement of anaerobic ammonium oxidation (anammox) and denitrification in intact sediment cores. *MEPS* **326**, 37-47 (2006).

33 Seeberg-Elverfeldt, J., Schlüter, M., Feseker, T. & Kölling, M. Rhizon sampling of porewaters near the sediment-water interface of aquatic systems. *Limnol. Oceanogr. Methods* **3**, 361-371 (2005).

34 Ibánhez, J. S. P. & Rocha, C. Porewater Sampling for NH_4^+ with Rhizon Soil Moisture Samplers (SMS): Potential Artifacts induced by NH_4^+ Sorption. *Freshw. Sci.* **33**, 1195-1203 (2014).

35 APHA-AWWA-WPCF. (eds AD Eaton, LS Clesceri, EW Rice, & AE Greenberg) (American Public Health Association, Washington D.C., 2005).

36 Lansdown, K. *et al.* Fine-Scale in Situ Measurement of Riverbed Nitrate Production and Consumption in an Armored Permeable Riverbed. *Environ. Sci. Technol.* **48**, 4425-4434 (2014).

37 McIlvin, M. R. & Altabet, M. A. Chemical conversion of nitrate and nitrite to nitrous oxide for nitrogen and oxygen isotopic analysis in freshwater and seawater. *Anal. Chem.* **77**, 5589 - 5595 (2005).

38 R: A Language and Environment for Statistical Computing (R Foundation for Statistical Computing, Vienna, Austria, 2014).

39 RStudio: Integrated development environment for R (RStudio, Boston, MA, 2012).

40 nlme: Linear and nonlinear mixed effects models (R package version 3.1-11, 2014).

41 Pinheiro, J. C. & Bates, D. M. *Mixed-effects models in S and S-Plus*. (Springer-Verlag, 2000).

42 vegan: Community ecology package (R package vesion 2.2-1, 2015).

43 Blanchet, F. G., Legendre, P. & Borcard, D. Forward selection of explanatory variables. *Ecology* **89**, 2623-2632 (2008).

44 Herlemann, D. P. R. *et al.* Transitions in bacterial communities along the 2000 km salinity gradient of the Baltic Sea. *ISME J.* **5**, 1571-1579, doi:10.1038/ismej.2011.41 (2011).

45 Long, A., Heitman, J., Tobias, C., Philips, R. & Song, B. Co-Occurring Anammox, Denitrification, and Codenitrification in Agricultural Soils. *Appl. Environ. Microbiol.* **79**, 168-176 (2013).

46 Caporaso, J. G. *et al.* QIIME allows analysis of high-throughput community sequencing data. *Nature Methods* **7**, 335-336 (2010).

47 Edgar, R. C. MUSCLE: multiple sequence alignment with high accuracy and high throughput. *Nucleic Acids Res.* **32**, 1792-1797 (2004).

48 Wang, Q., Garrity, G. M., Tiedje, J. M. & Cole, J. R. Naïve Bayesian Classifier for Rapid Assignment of rRNA Sequences into the New Bacterial Taxonomy. *Appl. Environ. Microbiol.* **73**, 5261-5267 (2007).

49 Tamura, K., Stecher, G., Peterson, D., Filipski, A. & Kumar, S. MEGA6: Molecular Evolutionary Genetics Analysis version 6.0. *Mol. Biol. Evol.* (2013).

50 Nei, M. & Kumar, S. *Molecular Evolution and Phylogenetics*. (Oxford University Press, 2000).

608 51 Le, S. Q. & Gascuel, O. An Improved General Amino Acid Replacement Matrix. *Mol.*
609 *Biol. Evol.* **25**, 1307-1320, doi:10.1093/molbev/msn067 (2008).
610 52 Felsenstein, J. Confidence Limits on Phylogenies: An Approach Using the Bootstrap.
611 *Evolution* **39**, 783-791 (1985).

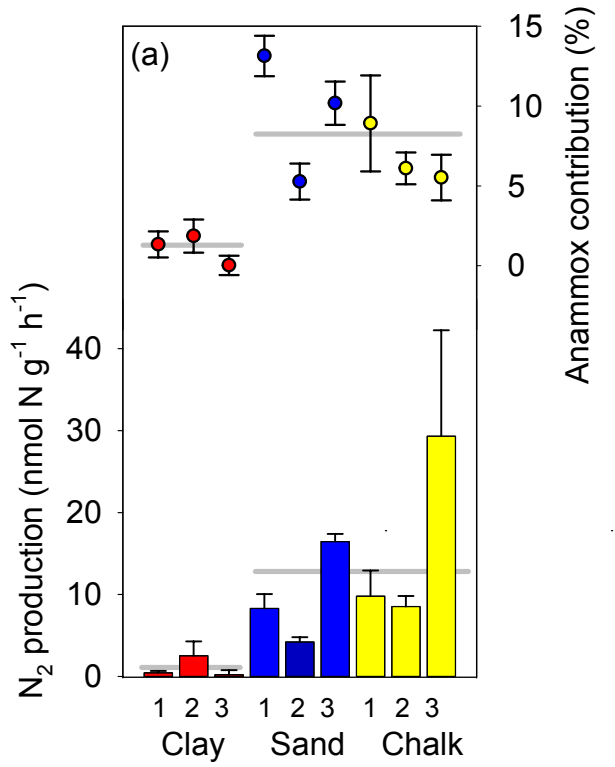
(a)
N_2 production (nmol N g^{-1} h^{-1})
Anammox contribution (%)
0
10
20
30
40
0
5
10
15
1 2 3 1 2 3 1 2 3
Clay
Sand
Chalk

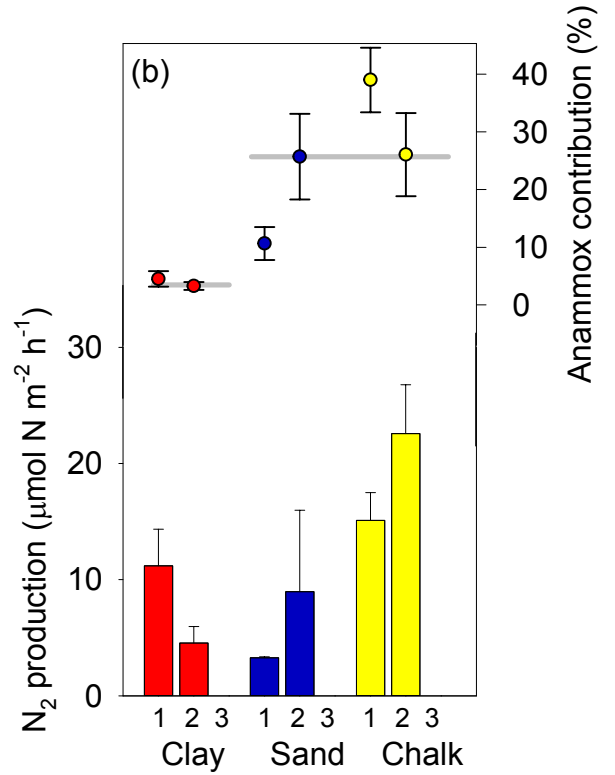
(b)
N_2 production (µmol N m^{-2} h^{-1})
Anammox contribution (%)
0
10
20
30
0
10
20
30
40
1 2 3 1 2 3 1 2 3
Clay
Sand
Chalk

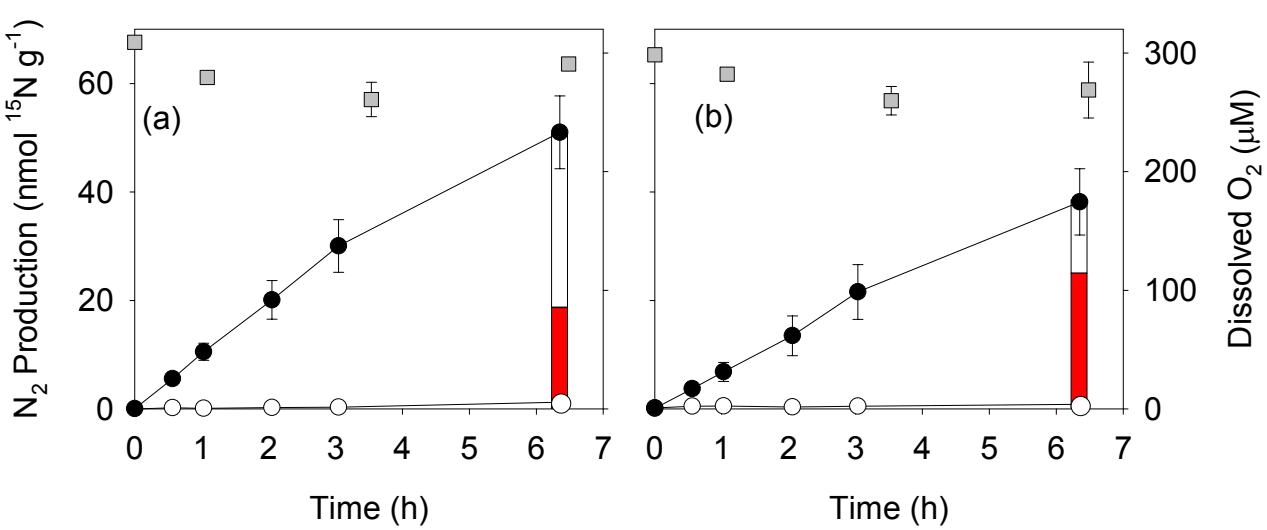
(a)
(b)
N_2 Production (nmol ^{15}N g^{-1})
Dissolved O_2 (μM)
Time (h)
Time (h)
0
20
40
60
100
200
300
0 1 2 3 4 5 6 7

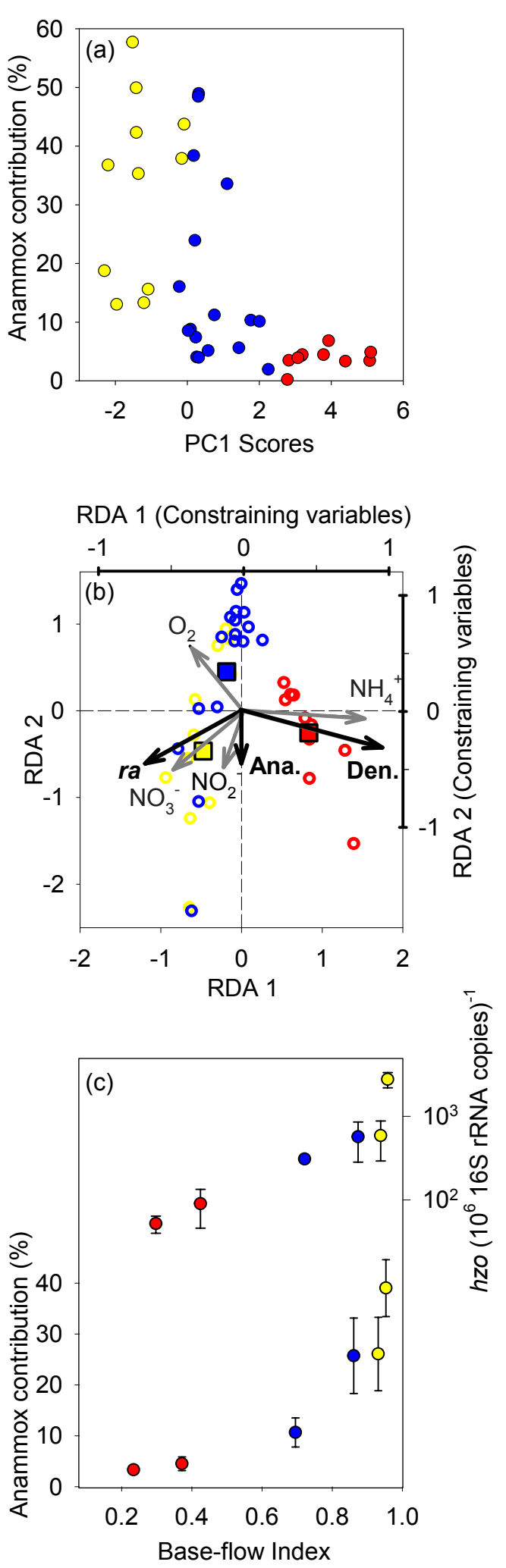
(a)
Anammox contribution (%)
PC1 Scores
(b)
RDA 1 (Constraining variables)
RDA 2
RDA 2 (Constraining variables)
RDA 1
O2
NH4+
ra
Ana.
Den.
NO2
NO3-
(c)
Anammox contribution (%)
hzo (10^6 16S rRNA copies)^-1
Base-flow Index